

Cellular Remodeling of HCO_3^- -Secreting Cells in Rabbit Renal Collecting Duct in Response to an Acidic Environment

Lisa M. Satlin and George J. Schwartz

Departments of Pediatrics and Physiology/Biophysics; Albert Einstein College of Medicine; Bronx, New York 10461

Abstract. The renal cortical collecting duct (CCD) consists of principal and intercalated cells. Two forms of intercalated cells, those cells involved in $\text{H}^+/\text{HCO}_3^-$ transport, have recently been described. H^+ -secreting cells are capable of apical endocytosis and have H^+ ATPase on the apical membrane and a basolateral $\text{Cl}^-/\text{HCO}_3^-$ exchanger. HCO_3^- -secreting cells bind peanut agglutinin (PNA) to apical membrane receptors and have diffuse or basolateral distribution of H^+ ATPase; their $\text{Cl}^-/\text{HCO}_3^-$ exchanger is on the apical membrane. We found that 20 h after acid feeding of rabbits, there was a fourfold increase in number of cells showing apical endocytosis and a numerically similar reduction of cells binding PNA. Incubation of CCDs at pH 7.1 for 3–5 h in vitro led to similar, al-

beit less pronounced, changes. Evidence to suggest internalization and degradation of the PNA binding sites included a reduction in apical binding of PNA, decrease in pH in the environment of PNA binding, and incorporation of electron-dense PNA into cytoplasmic vesicles. Such remodeling was dependent on protein synthesis. There was also functional evidence for loss of apical $\text{Cl}^-/\text{HCO}_3^-$ exchange on PNA-labeled cells. Finally, net HCO_3^- flux converted from secretion to absorption after incubation at low pH. Thus, exposure of CCDs to low pH stimulates the removal/inactivation of apical $\text{Cl}^-/\text{HCO}_3^-$ exchangers and the internalization of other apical membrane components. Remodeling of PNA-labeled cells may mediate the change in polarity of HCO_3^- flux observed in response to acid treatment.

THE renal collecting duct consists of two distinct cell types (15). Principal cells, accounting for two-thirds of all cells in the cortical collecting duct (CCD),¹ absorb Na^+ and secrete K^+ (16, 20, 33). Intercalated cells, comprising approximately one-third of all the cells in the CCD, are rich in carbonic anhydrase (12, 23) and mitochondria (15, 20). Since they show immunocytochemical evidence for H^+ ATPase (4, 6) and $\text{Cl}^-/\text{HCO}_3^-$ exchangers on opposite membranes (13, 25), and an alkaline cell pH (pH_i) (24, 27), they are believed to transport $\text{Cl}^-/\text{HCO}_3^-$. Two types of intercalated cells have been identified. H^+ -secreting cells possess apical H^+ ATPase (4, 5) and basolateral $\text{Cl}^-/\text{HCO}_3^-$ exchangers (13, 25). A characteristic feature of these cells is that they exhibit active and rapid endocytosis of the luminal membrane into acidic cytoplasmic vesicles (1, 5, 14, 26–28). Further, these vesicles can be stimulated in response to an increase in pCO_2 to fuse with the apical membrane, thereby inserting H^+ ATPases into that membrane

(1, 8, 14, 27). The predominant intercalated cell in the CCD secretes HCO_3^- by an apical $\text{Cl}^-/\text{HCO}_3^-$ exchanger, binds peanut agglutinin (PNA) to apical surface receptors (17, 25, 27, 28), does not have an apical H^+ ATPase (4, 6) and does not show apical endocytosis (27, 28).

The use of fluorescent dyes has allowed us to determine whether the polarity of intercalated cells can be altered by manipulating the pH of the environment to which they are exposed (27). Under baseline conditions, the isolated perfused rabbit CCD secretes HCO_3^- and is comprised primarily of HCO_3^- -secreting cells and few H^+ -secreting cells (27). Chronic acid loading of rabbits reverses the direction of net HCO_3^- transport from secretion to absorption and causes a 10-fold increase in number of H^+ -secreting cells and a numerically similar reduction in HCO_3^- -secreting cells. Since the total number of intercalated cells was not changed and no mitotic figures were observed, it is unlikely that cellular proliferation could mediate these changes (27). Thus, the increase in number of H^+ -secreting cells probably occurred at the expense of the HCO_3^- -secreting cells, thereby mediating the reversal in direction of HCO_3^- transport in the CCD (27).

It is the purpose of the present study to focus on the HCO_3^- -secreting cell and investigate some of the dynamic cellular changes that occur in response to an acid environment.

Abstracts of this work were presented at the 1987 Annual Meeting of the American Society for Clinical Investigation, San Diego; and at the 1987 and 1988 Annual Meetings of the American Society of Nephrology, in Washington, D.C., and in San Antonio, Texas.

1. *Abbreviations used in this paper:* BCECF, 2,7-bis-(2-carboxyethyl)-5 (and 6)-carboxyfluorescein; CCD, cortical collecting duct; PNA, peanut agglutinin; PNA-labeled, peanut agglutinin binding; Rh-BSA, rhodamine-BSA; 6-CF, 6-carboxyfluorescein.

Materials and Methods

Studies of Isolated Tubules

Mid-CCDs were dissected from renal medullary rays of New Zealand white female rabbits (1–2.5 kg) (24, 27, 28) in chilled dissection medium containing (in millimoles): 145 NaCl, 2.5 K_2HPO_4 , 2.0 $CaCl_2$, 1.2 $MgSO_4$, 4.0 Na lactate, 1.0 Na_3 citrate, 6.0 L-alanine, and 5.5 glucose, pH 7.4. Tubules were then transferred to an environmentally controlled specimen chamber, mounted on concentric pipettes, and perfused at 37°C (26–28).

Fluorescence Assays

Fluorescence assays were performed after an initial 20-min equilibration period at 37°C in which all tubules were perfused and bathed with an artificial solution simulating rabbit plasma (Burg's solution) (7, 27, 28) containing (in millimoles): 120 NaCl, 25 $NaHCO_3$, 2.5 K_2HPO_4 , 2.0 $CaCl_2$, 1.2 $MgSO_4$, 4.0 Na lactate, 1.0 Na_3 citrate, 6.0 L-alanine, and 5.5 glucose; the pH was 7.4 in 94% O_2 /6% CO_2 . Fluorescence labeling of intercalated cells with the pH sensitive dyes, 6-carboxyfluorescein(6-CF) (Fig. 1 *a*) and 2,7-bis-(2-carboxyethyl)-5 (and 6)-carboxyfluorescein (BCECF), the apical surface marker, rhodamine- or fluorescein-PNA (Fig. 1 *b*), and the endocytotic marker, rhodamine-BSA (Rh-BSA) (Fig. 1 *c*) was performed as previously described (3, 24, 27, 28).

Fluorescence Imaging

The numbers of endocytotic, PNA-labeled, and 6-CF or BCECF positive cells/millimeter tubular length were examined at 500 \times in a single, defined 200 μ m region of the perfused segment under epi-fluorescence (24, 28). The fluorescent profile of the apical PNA binding was generally linear (Fig. 1 *b*), enabling us to measure its length by ocular micrometry; we refer to this linear profile as a cap and the length as a PNA cap length. This measurement provided an estimate of the number of PNA-binding sites on the apical membrane of the PNA-labeled cell.

Excitation ratio microfluorometry of fluorescein, 6-CF or BCECF was used to measure pH in or around the cell. Instead of using a microspectrophotometer, as previously described (24, 26–28), we performed most studies with a silicon-intensified target video camera (model No. 66; Dage-MTI, Inc., Michigan City, IN) attached to the cine port of the microscope. Fluorescence images were visualized on a monitor (VMI 220; Hitachi Densi, Ltd., Woodbury, NY), and simultaneously recorded on VHS tape using a video cassette recorder (VHS Panasonic Omnivision II NV-8950, Panasonic Industrial Co., Secaucus, NJ).

The video-taped data were subsequently analyzed using a video photometric analyzer (model 204A; Instrumentation for Physiology and Medicine Inc., San Diego, CA) fed into a 2 channel chart recorder. One channel was used to record the fluorescent light intensity over a window placed on a PNA cap or within a cell. The other channel monitored background light intensity in a window of identical size placed at the periphery of the monitor

screen. The signal to background ratio generally exceeded 20:1, when compared to a window of identical size at the periphery of the monitor screen or to the cells before staining with the pH sensitive dyes.

Cell pH (pH_i)

PNA-labeled cells are believed to secrete HCO_3^- via apical Cl^-/HCO_3^- exchangers. To confirm the presence of these exchangers, we measured the change in pH_i in response to the removal of luminal Cl^- in individually identified PNA-labeled cells that stained brightly with BCECF or 6-CF. Tubules were studied initially with Burg's solution present in lumen and bath. The luminal perfusate was then replaced with Cl^- free perfusate containing (in millimoles): 110 Na gluconate, 25 $NaHCO_3$, 2.5 K_2HPO_4 , 4.0–8.0 Ca acetate (use of 4 mM or 8 mM calcium did not affect the magnitude of the change in pH_i in response to the removal of Cl^- [gluconate-containing solutions]), 1.2 $MgSO_4$, 4.0 Na lactate, 1.0 Na_3 citrate, 6.0 alanine, 5.5 glucose, pH 7.4 in 94% O_2 -6% CO_2 (27, 28). After 5–10 min, excitation ratio fluorometry was again repeated. Then, Burg's solution was restored to the lumen and, after 5–10 min, postexperimental measurements were performed; all excitation signals were recorded on videotape.

Transport Studies

CCDs were perfused and bathed in Burg's solution; the perfusion rates were 1–2 nl/min · millimeter tubular length. At least 3 collections of tubular fluid (6.6 nl each) were obtained during each experimental period for measurement of HCO_3^- concentration by microcalorimetry (Picapnotherm, Micro-analytic Instrumentation, Bethesda, MD) and calculation of net HCO_3^- transport (7, 27). Net HCO_3^- secretion was identified by a negative flux, while HCO_3^- absorption (equivalent to H^+ secretion) was denoted by a positive flux.

Experimental Protocols

Acid feeding of the rabbits was accomplished by nasogastric administration of a single dose of 15 mEq/kg NH_4Cl (which is converted to HCl by the liver) and limiting the rabbit's alkaline ash diet but not water to 30 gm/day. One group of rabbits received twice daily i.p. injections of actinomycin D (50 μ g/kg/d) beginning 2 d before acid feeding (19).

In vitro incubations were accomplished by perfusing the tubules for up to 5 h in a bath containing DME (Gibco Laboratories, Grand Island, NY) diluted (1:2) in either the HCO_3^- -free dissection medium or in Burg's solution, plus 1:300 penicillin and streptomycin (final concentration: 30 U/ml penicillin and 30 μ g/ml streptomycin; Gibco Laboratories), and 3% FCS in 94% O_2 /6% CO_2 . Control incubations were carried out at a HCO_3^- concentration of 25 ± 1 mM (pH 7.4 ± 0.1) and acidic incubations at a HCO_3^- concentration of 12 ± 1 mM (pH 7.1 ± 0.1) or 8 ± 1 mM (pH 6.9 ± 0.1).

At the completion of the incubation, the endocytosis assay was repeated and the numbers of endocytotically active, PNA-labeled, and doubly labeled

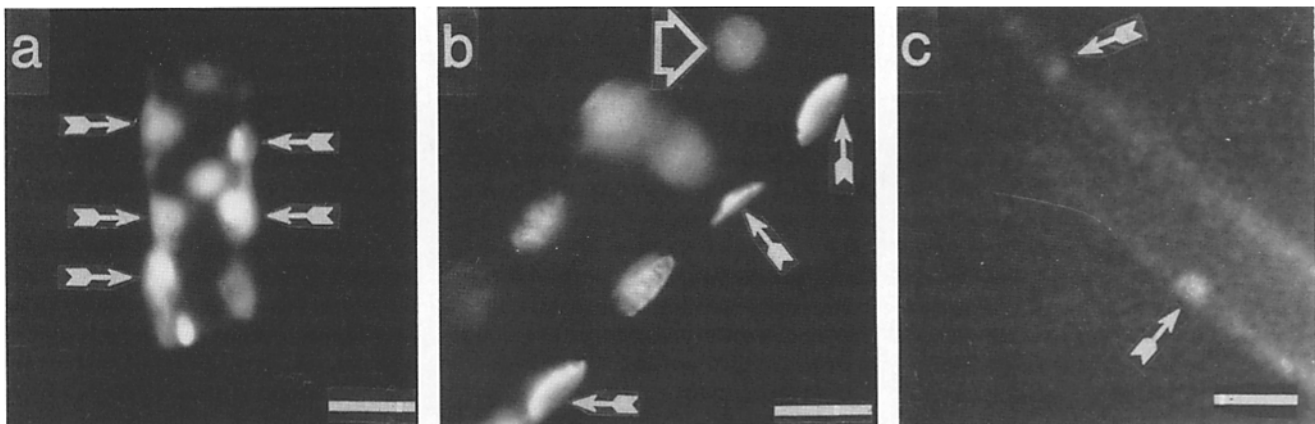


Figure 1. Functional fluorescent dyes in isolated perfused rabbit CCDs. (*a*) Tubule bathed in 20 μ M 6-CF diacetate to identify total number of intercalated cells (arrows). (*b*) Characteristic appearance of fluorescein-PNA in the CCD. Tubules isolated from normal animals bound PNA as a linear apical cap (arrow), or, when viewed *en face*, a punctate circular surface (arrowhead). (*c*) Fluid phase endocytosis (arrow) was evaluated by perfusing tubules with Rh-BSA during removal of ambient CO_2 (27, 28). Bar, (*a* and *c*) 30 μ m; (*b*) 20 μ m.

(PNA-labeled but now showing apical endocytosis) cells were counted in the same region of CCD.² The length of the fluorescent PNA profile was also remeasured. Cell viability was assessed by perfusion with 0.1% trypan blue for 1 min and, in some studies, exposure to 6-CF.

To trace the fate of the apical membrane binding PNA, the pH in the environment of the fluorescein-PNA cap was measured after the incubation in the presence of Burg's perfusate in lumen and bath. Also, the Cl⁻-dependent change in pH_i of PNA-labeled cells was used to document the effects of the prolonged incubation on apical Cl⁻/HCO₃⁻ exchange.³

HCO₃⁻ transport was measured during four periods of study: (a) preincubation baseline net HCO₃⁻ flux; (b) preincubation-stimulated HCO₃⁻ flux (using Cl⁻-free bath to achieve maximal HCO₃⁻ secretory rates) (27, 30); (c) postincubation baseline net HCO₃⁻ flux; and (d) postincubation stimulated HCO₃⁻ flux. (Initial 3-h incubations at pH 7.1 failed to reverse the direction of net HCO₃⁻ transport in isolated perfused CCDs. We therefore chose to lower the pH for the acid incubation to 6.9 to maximize the tubular response.)

Cycloheximide (5 μg/ml) or actinomycin D (1 μg/ml) was added to the bath in those experiments designed to inhibit protein synthesis or DNA transcription, respectively (10).

Electron Microscopy

CCDs were perfused with 50 μg/ml PNA coupled to peroxidase (arachis hypogaea, peroxidase, type VI labeled; Sigma Chemical Co., St. Louis, MO) for 30 min at room temperature. After a 15-min luminal rinse, the segment was incubated under control or acidic conditions for 2 h. Tubules were then prepared for transmission EM as previously described (28). Ultrathin sections (~80 nm) were cut on a microtome (ultracut E; Reichert Scientific Instruments, Buffalo, NY). Sections were stained with uranyl acetate followed by lead citrate and viewed on an electron microscope (1200 EX; JEOL USA, Cranford, NJ).

Statistics

Results are expressed as mean ± SEM (number of animals or cells). Multiple comparisons of unpaired data were performed using an analysis of variance plus the multiple range test (24, 29). Significance was asserted if *p* < 0.05.

2. Fluorescein PNA staining was well preserved during the prolonged incubations provided the tubules were exposed to a minimal amount of ambient light. No difference in the apical fluorescent profile was observed when fluorescein-PNA was reperfused after prolonged incubation at pH 7.4 (data not shown).

3. Preliminary experiments were performed to determine whether PNA binding, per se, inhibited Cl⁻/HCO₃⁻ exchange. To this end, the change in pH_i in response to luminal Cl⁻ removal was measured in cells labeled with PNA at the outset of the experiment. Under these experimental conditions, mean pH_i increased by 0.38 ± 0.15 pH units, from 7.53 ± 0.07 to 7.91 ± 0.09 (*n* = 6 cells; *p* < 0.05), an increase that was not statistically different from that observed when cells were labeled with PNA after performing the postincubation pH_i measurements.

Results

Remodeling of HCO₃⁻-Secreting Cells by Short Term In Vivo Acid Feeding

Previously, we had shown that long term acid feeding causes an increase in number of H⁺-secreting cells and a concomitant decrease in number of HCO₃⁻-secreting cells (27). We now show that acid feeding as a single dose results in similar cellular changes within 20 h. When the animals were fed acid, the concentration of HCO₃⁻ in the blood and the pH of the urine declined within 5 h, but recovered to normal levels by 20 h (Table I).

In CCDs examined 20 h after acid feeding, there was an increase in number of cells showing apical endocytosis, a change that was nearly identical to the decrease in number of PNA-labeled cells (Table I). (We did not systematically look for doubly stained [endocytotic/PNA-labeled] cells at the time these experiments were performed.) Moreover, ~50% of the PNA-labeled cells showed fluorescent profiles of markedly reduced length (<6 μm) (Fig. 2). On the other hand, CCDs isolated from rabbits 5 h after acid loading showed a small but insignificant increase in number of cells exhibiting apical endocytosis (Table I).

To test for the presence of apical Cl⁻/HCO₃⁻ exchange in PNA-labeled cells, we measured the reversible increase in pH_i in response to the removal of luminal Cl⁻. The increment in pH_i in CCDs taken from normal rabbits was reversible and averaged 0.35 ± 0.07 pH units above the baseline (*p* < 0.01, paired *t* test) (Fig. 3 a), consistent with the presence of apical Cl⁻/HCO₃⁻ exchangers in PNA-labeled cells. In CCDs taken from rabbits 20 h after acid feeding, the change in pH_i in response to luminal Cl⁻ removal was examined separately in cells having small PNA profiles (<6 μm) and in those having linear PNA caps typical of the untreated cells (>8 μm) (Figs. 1 b and 2). The increment in pH_i in cells having small PNA profiles was -0.01 ± 0.10 (*n* = 8 cells in 5 CCDs) (Fig. 3 c) compared with 0.35 ± 0.12 in cells with typical caps (*n* = 5 cells in 5 CCDs, *p* < 0.05) (Fig. 3 b). Baseline pH_i did not differ between cells with small PNA caps (7.35 ± 0.11) and normal caps (7.32 ± 0.17, *p* = NS). The increase in pH_i in cells with typical PNA caps from acid-loaded and control animals did not differ (Figs. 3 a and b).

Previously, we found that brief exposure of CCDs to 6-CF diacetate preferentially labeled intercalated cells (24, 27, 28),

Table I. Effects of Acid Feeding In Vivo on Isolated Perfused Rabbit Cortical Collecting Ducts

Maneuver	Whole animal data		Cells/mm cortical collecting duct		
	Urine pH	Plasma HCO ₃ ⁻ (mM)	PNA-labeled	Apical endocytotic	Total intercalated*
Control	8.3 ± 0.1 (7)	27.5 ± 0.8 (6)	152 ± 8 (9)	11 ± 6 (7)	157 ± 7 (8)
5-h acid fed	4.6 ± 0.1 (4) ^{‡§}	17.8 ± 1.4 (6) ^{‡§}	129 ± 7 (4)	29 ± 15 (5)	145 ± 6 (5)
20-h acid fed	8.0 ± 0.1 (8)	29.4 ± 0.8 (9)	109 ± 7 (4) [‡]	44 ± 6 (8) [‡]	148 ± 6 (6)
20-h acid fed + Actinomycin D	4.7 ± 0.1 (5) ^{‡§}	13.8 ± 2. (5) ^{‡§}	149 ± 7 (5) [§]	13 ± 9 (5) [§]	137 ± 9 (5)

Mean ± SEM; *n* = number of animals.

* Intercalated cells were identified by preferential staining after a short exposure to 6-CF.

[‡] *p* < 0.01 compared to control.

[§] *p* < 0.01 compared to 20-h acid fed.

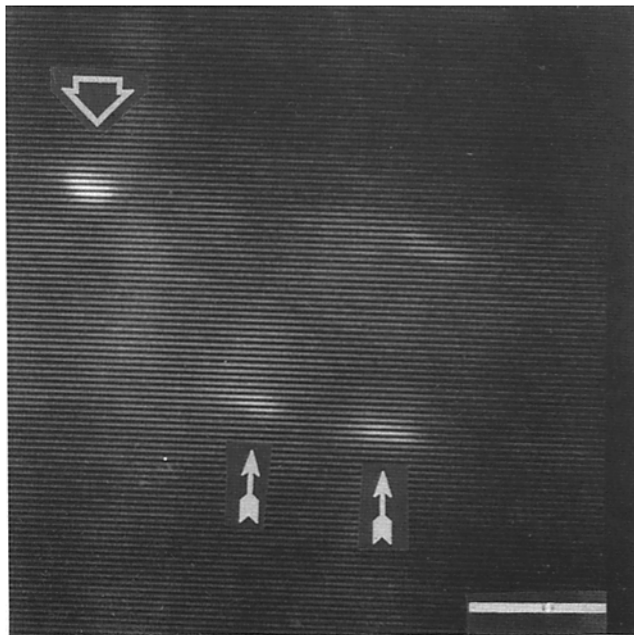


Figure 2. Fluorescence micrograph of a CCD isolated from a rabbit 20 h after acid feeding and perfused with rhodamine-PNA. Note the presence of both typical (*arrow*) and small (*arrowhead*) PNA-labeled profiles in this tubule. Bar, 20 μ m.

and using this method we noted no change in the total number of intercalated cells after short term acid feeding (Table I). These results demonstrate that PNA-labeled cells undergo a remodeling process that includes an induction of apical endocytosis, a reduction in number or affinity of PNA binding sites, and inhibition or degradation of apical $\text{Cl}^-/\text{HCO}_3^-$ exchangers. This remodeling process is slow but occurs well within 20 h after acid feeding of the rabbits.

Remodeling of HCO_3^- -Secreting Cells by In Vitro Incubation in Acidic Medium

To test whether such cellular remodeling is mediated simply by a low extracellular pH or by hormonal or neural responses

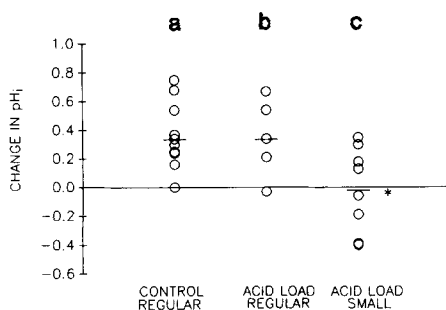


Figure 3. The change in pH_i of individual PNA-labeled cells in response to luminal Cl^- removal. Regular or typical PNA caps were studied in CCDs isolated from rabbits (*a*) after no incubation, and (*b*) 20 h after acid feeding. Small PNA caps were found only in the acid-treated group (*c*). Mean values for each of the three groups are depicted by the short horizontal lines. Regular PNA caps in both control and acid fed groups showed an increase in pH_i of 0.35 pH units in response to the removal of luminal Cl^- . A significantly smaller change in pH_i (-0.01 ± 0.10) in response to this same maneuver was observed in the group of small caps.

Table II. Effects of Incubation in Acidic Medium on Isolated Perfused Rabbit Cortical Collecting Ducts

	Cells/mm tubule			
	PNA labeled		Apical endocytotic	
	pre	post	pre [†]	post [†]
5-h control	139 \pm 8	133 \pm 9 (6)	9 \pm 3	11 \pm 3 (6)
3-h acid	142 \pm 6	131 \pm 5 (8) [‡]	11 \pm 3	36 \pm 6 (7) ^{‡§}
5-h acid	147 \pm 4	132 \pm 6 (9) [*]	6 \pm 4	31 \pm 3 (12) ^{‡§}
5-h acid + cycloheximide	130 \pm 11	118 \pm 11 (4) [*]	5 \pm 5	2 \pm 1 (4)

Mean \pm SEM; *n* = number of animals.

^{*} *p* < 0.05 compared to *pre* value by paired *t* test.

[‡] *p* < 0.01 compared to *pre* value by paired *t* test.

[§] *p* < 0.05 compared to control value.

^{||} PNA-labeled cells showing apical endocytosis were not seen before incubation.

[†] Includes cells only showing apical endocytosis plus those PNA-labeled cells that developed apical endocytosis.

to acid feeding in vivo, we investigated whether cellular remodeling occurs in CCDs exposed to low extracellular pH in vitro. By using Rh-BSA as an endocytotic marker and fluorescein-PNA as a surface marker both before and after the incubation, we were able to determine whether PNA-labeled cells could be induced to exhibit apical endocytosis. After only 3 h of incubation in an acidic medium (pH 7.1), we found a threefold increase in the number of cells exhibiting apical endocytosis (Table II). This was associated with a 10% reduction in the number of PNA-labeled cells (Table II); 28 \pm 6 of the endocytotically active cells/millimeter of tubular length simultaneously possessed apical PNA caps (Fig. 4).⁴ These cells excluded trypan blue and stained intensely with 6-CF (not shown). The increase in number of cells showing apical endocytosis and decrease in number of PNA-labeled cells was sustained at 5 h of incubation in acidic medium (Table II); by this time only 11 \pm 5 cells/millimeter were doubly labeled. We found that incubation in acidic medium had no effect on total number of intercalated cells (179 \pm 15 vs. 161 \pm 9; *p* = NS). Time controls showed no significant changes (Table II).

To test whether decreased apical binding of PNA after acid treatment is the result of internalization of the PNA receptor-ligand complex, we studied the fate of bound PNA after short term incubation in vitro. We first measured the length of the PNA profile in 6–11 cells/CCD to estimate the number of apical surface binding sites on these cells. Before incubation this length averaged 10.0 \pm 0.5 μ m. Incubation in acidic medium (3 h) caused a significant reduction in length from the preincubation values ($-34.8 \pm 4.3\%$) (Figs. 5 *a* and 6, *a* and *b*). Indeed, PNA caps <4 μ m in length, appearing as brightly fluorescent “dots,” were frequently seen after incubation in acidic medium (Fig. 6 *c*). Incubation at pH 7.4 led to much smaller changes (Fig. 5 *a*).

This result suggests that PNA binding sites were being internalized and even degraded, perhaps in acidic cytoplasmic compartments. We therefore used the pH sensitivity of fluorescein coupled to PNA to determine whether this marker

4. Although addition of lectins can induce receptor-mediated endocytosis in other cell systems (11), we do not believe that this is responsible for the cellular remodeling observed after incubation at low pH. The reason for this is that perfusion of the lectin failed to induce endocytosis at pH 7.4 (Figs. 5 and 6).

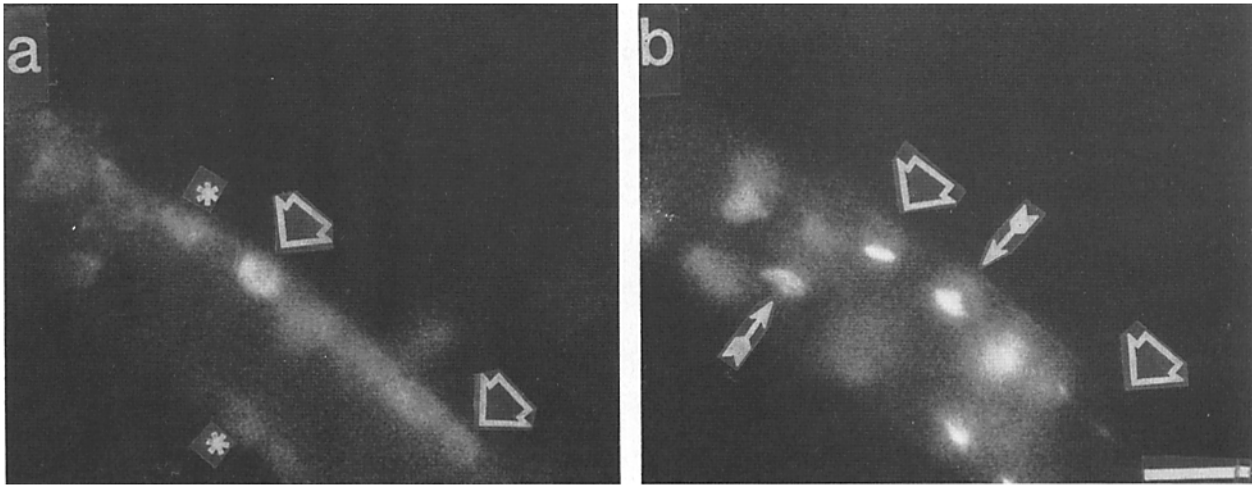


Figure 4. Fluorescence micrographs of a single CCD perfused *in vitro* for 5 h under conditions of low ambient pH. *a* shows endocytosis of Rh-BSA and (*b*) fluorescein-PNA binding. Note the doubly stained cells (i.e., endocytotic cells that also possess apical PNA caps) designated by arrowheads at identical locations in *a* and *b*. Other cells that stain solely with Rh-BSA or fluorescein-PNA, are designated by asterisks in *a* and arrows in *b*, respectively. In *b*, apical PNA staining appears diffuse in some cells; at higher magnification (not shown), subapical fluorescence is evident, suggesting that the PNA cap is being removed from the membrane by endocytosis. Bar, 20 μ m.

entered such a compartment. After 3 h incubation in acidic medium, the pH in the environment of the fluorescein PNA was significantly reduced from 7.4 to 6.77 ± 0.14 pH units (Fig. 5 *b*). The brightly fluorescent PNA “dots” described above were consistently more acidic, averaging only 6.10 ± 0.15 pH units (11 PNA “dots” studied in 5 tubules). Tubules incubated at pH 7.4 did not show a significant decrease in pH in the area of the PNA (Fig. 5 *b*).

Further confirmation of internalization of PNA was documented by transmission electron microscopy where we found that after exposure to acidic media abundant membrane bound reaction product was now seen in numerous endocytotic vesicles (Fig. 7, *c* and *d*, arrows); also, some reaction product was still bound to the apical membrane (Fig. 7 *c*). In contrast, after incubation at pH 7.4, most of the reaction product was found on the luminal surface and little in cytoplasmic vesicles (Fig. 7, *a* and *b*). These results indicate that PNA binding sites were internalized in response to incubation at low pH; we cannot as yet determine whether these sites were subsequently degraded.

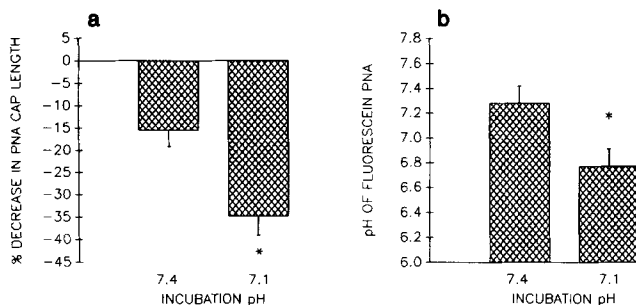


Figure 5. Effect of 3–5-h incubation (pH 7.4 and pH 7.1) on fate of PNA caps. (*a*) Mean decrease in length of PNA profile (apical length; in micrometers), expressed as the percentage change from preincubation values. (*b*) Fluorescein PNA pH measured in the environment around the PNA at the conclusion of the incubations. Results are expressed as means (hatched bars) +1 SEM. *n* = number of tubules. *, $p < 0.05$ compared to control incubation (pH 7.4).

The apical membrane of HCO_3^- -secreting cells contains not only PNA binding sites, but also $\text{Cl}^-/\text{HCO}_3^-$ exchangers. To test whether low ambient pH also affects this anion exchanger, we assessed its function by measuring pH_i in the presence and absence of Cl^- . In untreated PNA-labeled cells, we observed a reversible increase in pH_i in every tubule immediately after equilibration (no incubation) (Fig. 8 *a*). The pH_i of PNA-labeled cells averaged 7.40 ± 0.10 in the presence of Cl^- (Burg’s solution), increasing by 0.43 ± 0.09 pH units to 7.82 ± 0.09 ($n = 5$ tubules; $p < 0.01$) after removal of luminal Cl^- . The increase in pH_i for 15 out of 18 (83%) cells examined in the five tubules exceeded 0.2 pH units (Fig. 9 *a*).

After 3 h of incubation at pH 7.1, the increase in pH_i in PNA-labeled cells in response to Cl^- removal from the lumen was blunted, averaging only 0.16 ± 0.02 pH units; pH_i increased from 7.44 ± 0.10 to 7.59 ± 0.10 ($n = 6$ tubules; $p < 0.005$) (Fig. 8 *c*). This degree of alkalization was significantly less than that observed after 3 h incubation at pH 7.4 or in nonincubated tubules ($p < 0.05$) (Figs. 8, *a* and *b*).

Since not every PNA-labeled cell would be expected to remodel after only 3 h incubation in acidic medium and the distribution of individual pH_i changes after Cl^- removal did not always appear to be normal (Fig. 9), nonparametric analysis (29) of the individual cellular responses to luminal Cl^- removal was also performed. After a 3-h incubation at pH 7.4, almost all PNA-labeled cells showed significant $\text{Cl}^-/\text{HCO}_3^-$ exchange; pH_i increased by ≥ 0.2 pH units in $>80\%$ of these cells (Fig. 9 *b*), just as observed after no incubation period (Fig. 9 *a*). In contrast, after 3 h of incubation in acidic medium only 6 out of 15 cells (40%) showed an increase in pH_i of ≥ 0.2 pH units ($X^2 = 6.22$; $p < 0.025$) (Fig. 9 *c*). Moreover, ranking of the individual cellular responses after the 3-h incubations demonstrated that acidic incubation significantly reduced the magnitude of $\text{Cl}^-/\text{HCO}_3^-$ exchange ($p < 0.01$, Mann-Whitney test).

To determine if exposure to acid and the changes described above resulted in a reversal of polarity of HCO_3^- flux, we measured net HCO_3^- transport in perfused CCDs both be-

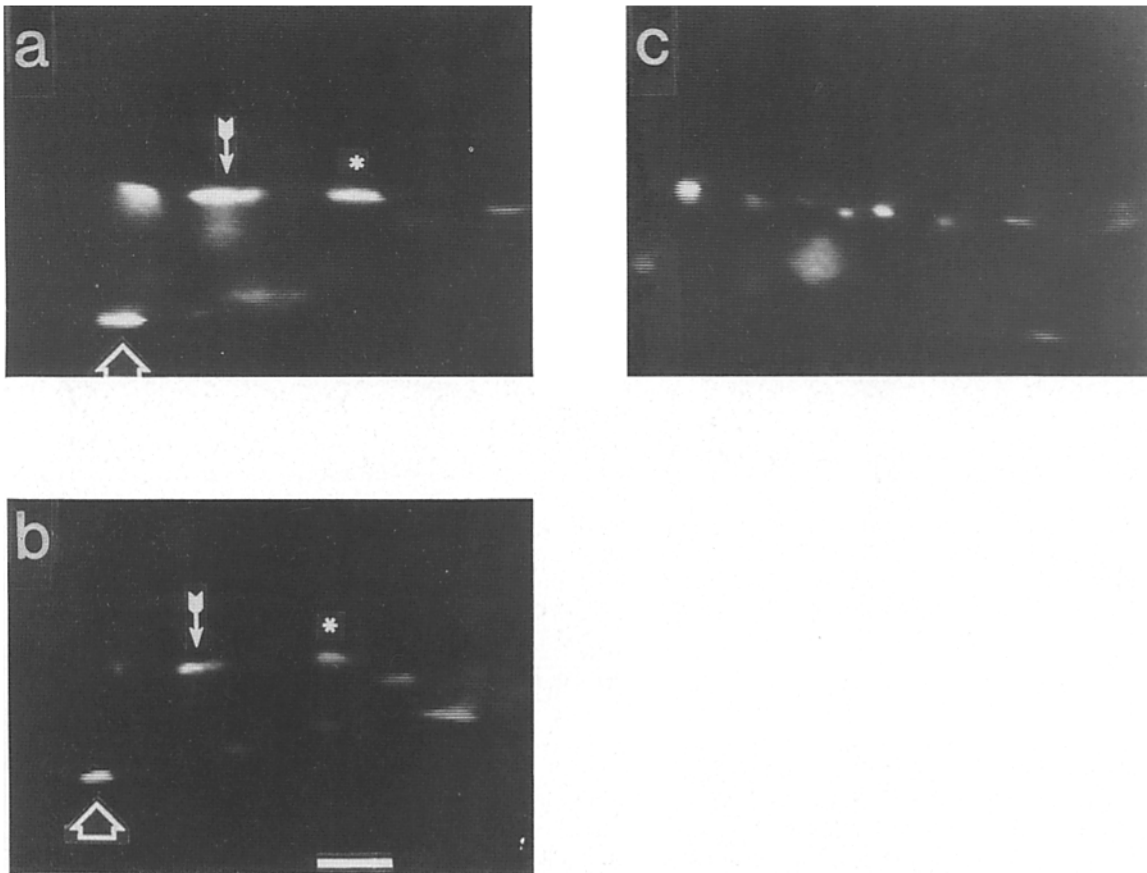


Figure 6. (a and b) Fluorescence micrographs of a single region of a CCD before (a) and after (b) a 3-h incubation at pH 7.1. Each symbol identifies a specific PNA cap in a and b. Note the shortening of the fluorescent caps over time. (c) Numerous fluorescent PNA "dots" are seen in another CCD after incubation in acidic medium. Bar, 20 μm .

fore and after exposure to 3–4 h of low pH (pH 6.9) in luminal and bathing solutions. We found that net HCO_3^- transport converted from secretion to absorption (pre: -2.82 ± 0.76 pmol/min · millimeter; post: $+1.91 \pm 0.58$, $p < 0.001$, paired *t* test) (Fig. 10 b). Also, the maximal rate of HCO_3^- secretion fell in each of the four tubules (pre: -14.51 ± 4.16 pmol/min · millimeter; post: -6.61 ± 1.83 , $0.05 < p < 0.10$, paired *t* test) (Fig. 11 b). There was no change in baseline or maximal rates of HCO_3^- secretion after incubation at pH 7.4 (Figs. 10 a and 11 a).

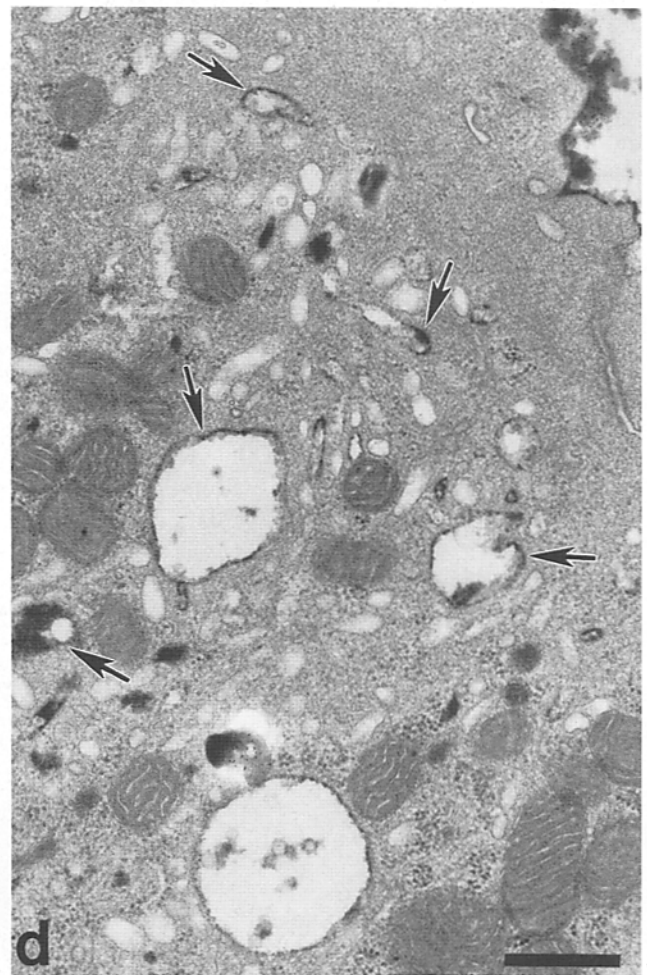
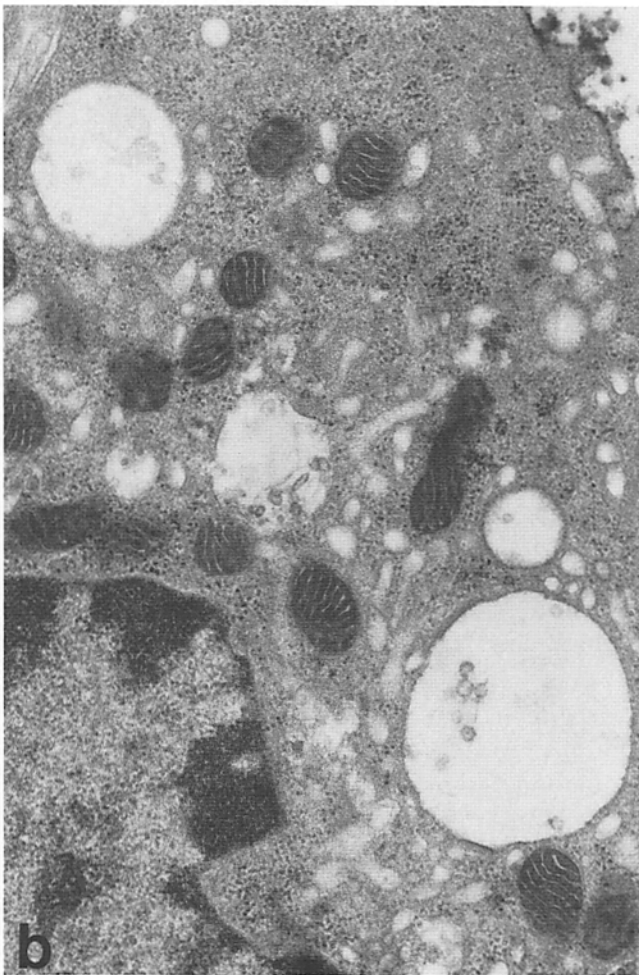
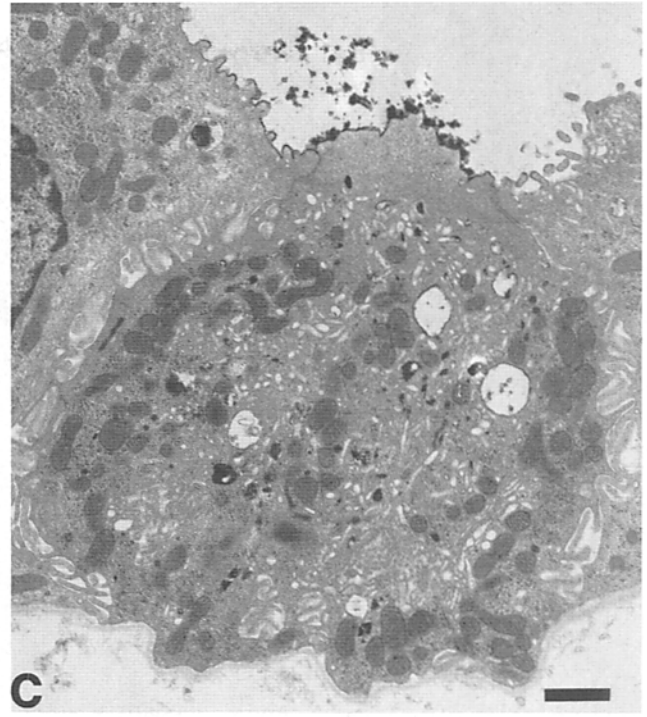
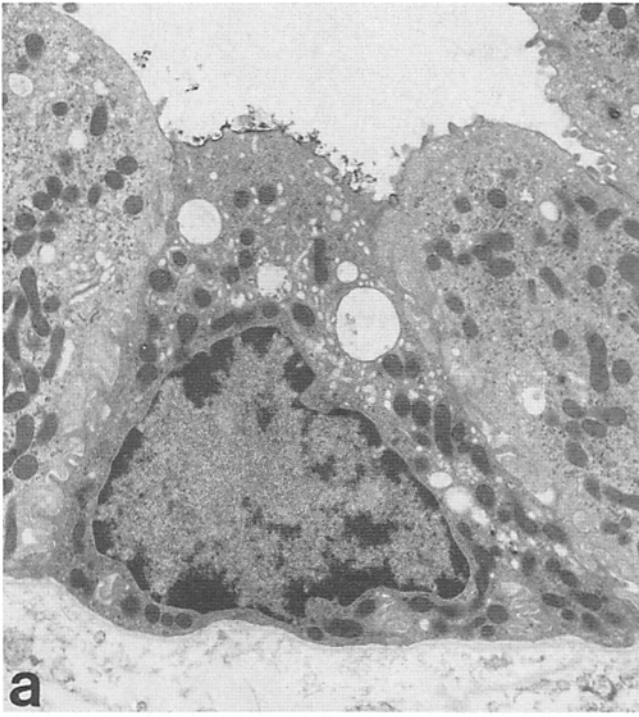
To test the integrity of the perfused epithelium, we measured transepithelial voltage (26) generated by the CCD before and after the long incubation. Control tubules averaged -11 ± 3 mV before and -13 ± 2 mV after the 3–4-h incubation at pH 7.4 (mean change = 2 ± 3 mV; $n = 8$, $p = \text{NS}$). Similarly, tubules averaged -6 ± 1 mV before and -6 ± 2 mV after the incubation at pH 7.1 (mean change = 0 ± 2 mV, $n = 11$, $p = \text{NS}$). Further, the integrity of the tight junctions between cells was evident at the electron micro-

scopic level (Fig. 7 c). These results suggest that tight junctions remain intact in the CCD throughout the experiment.

Effect of Protein Synthesis Inhibitors on Cellular Remodeling

The responses described above are pleiotropic and include inhibition or degradation of $\text{Cl}^-/\text{HCO}_3^-$ exchangers, induction of apical endocytosis, and internalization of PNA binding sites. To test whether these complex responses require *de novo* protein synthesis, we tested the effects of cycloheximide and actinomycin D on some of these changes. We measured endocytosis by perfusing with Rh-BSA and found that whereas acidic incubation *in vitro* stimulated apical endocytosis, concomitant exposure to cycloheximide completely blocked the endocytotic response (Table II). Similarly, actinomycin D given to the animals prevented the induction of apical endocytosis resulting from acid feeding (Table I). We were unable to use actinomycin D *in vitro* because of cell

Figure 7. Transmission electron micrographs of intercalated cells in CCDs perfused with peroxidase lectin and incubated for 2 h at pH 7.4 (a and b) and pH 7.1 (c and d). Intercalated cells are characterized by numerous mitochondria, the absence of basolateral infoldings, and a microvillated surface (15, 20, 32). Both intercalated cells retain electron dense PNA label on their luminal surfaces. Very little reaction product is seen in the cytoplasm of the intercalated cell incubated at pH 7.4 (a and b) whereas abundant electron-dense material is observed throughout the cytoplasm in the cell exposed to low pH (c and d). In d, after acidic incubation, peroxidase lectin is seen to be present in membrane bound endocytotic vesicles (arrows). Bar, (a and c) 1.0 μm ; (b and d) 0.5 μm .



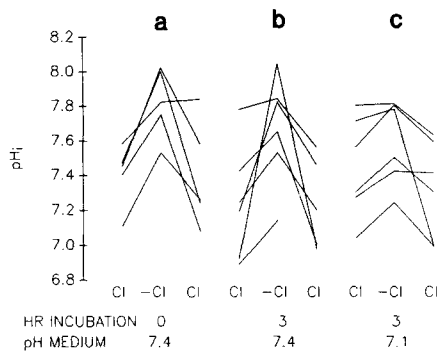


Figure 8. Effect of luminal Cl^- removal ($-\text{Cl}$) on pH_i of PNA-labeled cells in CCDs exposed to (a) no incubation, pH 7.4, (b) 3-h incubation, pH 7.4, and (c) 3-h incubation, pH 7.1. Each line connects the mean measurements for all PNA-labeled cells examined in a given tubule.

sloughing that was regularly seen 2–3 h into the incubation. We cannot explain the observation that actinomycin D did, and cycloheximide did not, prevent the decrease in number of PNA-labeled cells (Tables I and II). It is interesting to note that actinomycin D-treated animals fed acid were unable to excrete the acid as well as acid-fed animals that did not receive this inhibitor (Table I), suggesting that the reversal of polarity of HCO_3^- transport plays a critical role in regulating acid-base balance. These results indicate that the complex cellular response to acid treatment requires the synthesis of one or several proteins.

Discussion

The response of the CCD to *in vivo* acid loading includes an increase in number of cells active in apical endocytosis (H^+ -secreting cells) and a numerically similar reduction in number of PNA-labeled (HCO_3^- -secreting) cells. These results indicate that the reversal in direction of net transport in the CCD from that of HCO_3^- secretion to that of HCO_3^- absorption (equivalent to H^+ secretion) (18, 21, 22, 27), observed in response to *in vivo* and *in vitro* acid treatment is

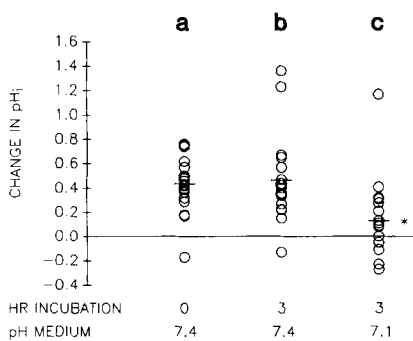


Figure 9. The change in pH_i of individual PNA-labeled cells in response to luminal Cl^- removal. Collecting ducts were exposed to (a) no incubation, pH 7.4; (b) 3-h incubation, pH 7.4; and (c) 3-h incubation, pH 7.1. Mean values for each of the three conditions are depicted by the horizontal lines. Note that most of the PNA-labeled cells (>80%) studied at pH 7.4 (a and b) showed an increase in pH_i of ≥ 0.2 pH units in response to the removal of luminal Cl^- . (c) Only a minority (40%) of cells studied after incubation at low pH showed this degree of alkalization in response to the same maneuver.

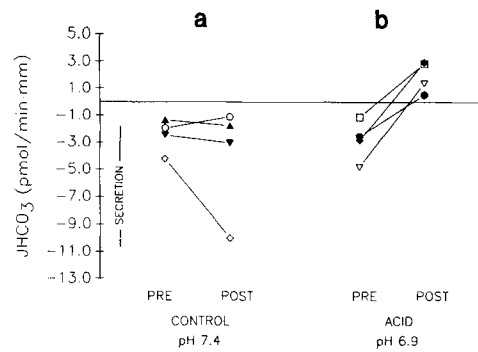


Figure 10. The effect of 3–4 h (a) control (pH 7.4) and (b) acid (pH 6.9) incubations on baseline net HCO_3^- transport (pmol/min·mm) in isolated perfused CCDs. “Pre” values denote the HCO_3^- transport rates in individual tubules before the incubation; “post” values for the same CCDs were obtained after the incubation. Baseline HCO_3^- transport measurements were performed with Burg’s solution present in lumen and bath. Each symbol represents data from a single CCD.

mediated in large part by an increase in number and/or activity of H^+ -secreting cells at the expense of a decrease in number and/or activity of HCO_3^- -secreting cells.

We suggest that remodeling of the PNA-labeled cell represents an initial process involved in the conversion of some HCO_3^- -secreting cells to H^+ -secreting cells. At a minimum, for a HCO_3^- -secreting cell to reverse its functional polarity to become that of an H^+ -secreting cell, the following cellular changes must occur: $\text{Cl}^-/\text{HCO}_3^-$ exchangers must be removed from the apical membrane, newly synthesized band 3-like $\text{Cl}^-/\text{HCO}_3^-$ exchangers need to be inserted into the basolateral membrane, and H^+ ATPases must be removed from the basolateral membrane and be inserted into the apical membrane. Thus far, we have shown that acid treatment reduced apical $\text{Cl}^-/\text{HCO}_3^-$ exchange and induced apical endocytosis. We propose that the induction of apical endocytosis in remodeling PNA-labeled cells reflects the insertion of H^+ ATPases into the apical membrane, because the cytoplasmic vesicles that acidified the fluorescein-PNA now have

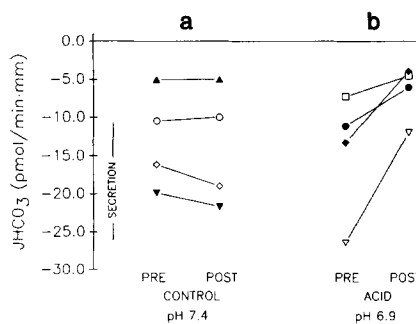


Figure 11. The effect of 3–4 h (a) control (pH 7.4) and (b) acid (pH 6.9) incubations on maximal net HCO_3^- transport (pmol/min·mm) in isolated perfused CCDs. “Pre” values denote the HCO_3^- transport rates in individual tubules before the incubation; “post” values for the same CCDs were obtained after the incubation. Maximal HCO_3^- transport measurements were achieved with Burg’s solution present in lumen and Cl^- free perfusate in the bath (27, 30). Each symbol represents data from the same CCDs depicted in Fig. 10.

access to the luminal fluid. Since the total number of intercalated cells did not change after acid treatment, yet the direction of net HCO_3^- transport reversed, HCO_3^- -secreting cells must have remodeled to form H^+ -secreting cells. Clearly, immunocytochemical studies are needed to show that an apical H^+ -ATPase and basolateral $\text{Cl}^-/\text{HCO}_3^-$ exchanger are now present on the newly remodeled cell.

The nature of the apical glycoprotein that binds PNA and its precise relationship to the apical $\text{Cl}^-/\text{HCO}_3^-$ exchanger, if any, remains unclear. The basolateral, but not the apical, anion exchange protein is immunocytochemically similar to erythrocyte band 3 (13, 25); however, basolateral PNA binding has not been demonstrated in intercalated cells of the rabbit kidney (17, 25), indicating that the PNA binding protein is not band 3. The apical exchanger may be related to band 3, because several mRNA transcripts can be identified by probing kidney RNA with a band 3 cDNA at low stringency (2).

What is the signal that induces internalization of the PNA cap and inactivation/removal of apical $\text{Cl}^-/\text{HCO}_3^-$ exchangers? That this remodeling occurred *in vitro* indicates that it was not attributable to neural, humoral, or other changes induced by acid feeding *in vivo*. Rather, an alteration of the cellular milieu mediated these changes. Specifically, CO_2 causes an intracellular acidosis that in turn elevates cell calcium, resulting in exocytosis of proton pumps (8, 31). In the present experiments, a transient intracellular acid load resulting from the reduction of ambient HCO_3^- concentration may have increased cell calcium, in turn changing cytoskeletal organization and stimulating cellular remodeling. On the other hand, a low cytoplasmic pH inhibits endocytosis and transport from the Golgi network (9). Therefore, it is interesting to note that the steady state pH_i in PNA-labeled cells tended to be higher after incubation in acidic medium compared to after control incubation (Figs. 8, *b* and *c*). Inactivation of apical $\text{Cl}^-/\text{HCO}_3^-$ exchange may have caused a rise in PNA-labeled cell pH_i as H^+ pumping continued at the basolateral membrane and generated intracellular base. Further, the results of the protein synthesis inhibitors indicate that the process of remodeling is complicated and may require the synthesis of one or more proteins.

Of course, it is conceivable that cells do not change polarity, but that the function of HCO_3^- -secreting cells is inhibited, whereas that of H^+ -secreting cells is greatly stimulated. Experiments to document that newly endocytotically active cells secrete H^+ are necessary to address this question.

The observation that the direction of epithelial HCO_3^- transport can be altered in response to an environmental stimulus provides a potential system for learning more about the developmental biology of such transport systems. For example, the removal of an anion exchange protein from the apical membrane and insertion of a slightly different anion exchanger (with a different signal sequence) into the basolateral membrane in response to acidic conditions may reveal much about the development of cell polarity. Finally, remodeling of the PNA-labeled cells described here may help us to understand more about intracellular sorting of specific transport proteins (H^+ pumps, $\text{Cl}^-/\text{HCO}_3^-$ exchangers) to the apical or basolateral membranes.

We would like to thank B. Zavilowitz and Dr. F. Mehrgut for technical assistance, Mr. F. Macaluso of the Albert Einstein College of Medicine An-

alytical Ultrastructure Center for preparing the electron micrographs, and Dr. A. Spitzer for his support and encouragement of these studies.

L. M. Satlin was supported by a National Institutes of Health (NIH) First Award AM-38470. G. J. Schwartz was supported by an NIH grant HD-13232 and is an Established Investigator of the American Heart Association; funds were contributed in part by the New York Chapter.

Received for publication 9 January 1989 and in revised form 30 May 1989.

References

- Al-Awqati, Q. 1986. Proton-translocating ATPases. *Annu. Rev. Cell Biol.* 2:179-199.
- Alper, S. L., R. Kopito, S. M. Libresco, and H. F. Lodish. 1988. Cloning and characterization of a murine band 3-related cDNA from kidney and from a lymphoid cell line. *J. Biol. Chem.* 263:17092-17099.
- Alpern, R. J. 1985. Mechanism of basolateral membrane $\text{H}^+/\text{OH}^-/\text{HCO}_3^-$ transport in the rat proximal convoluted tubule. *J. Gen. Physiol.* 86: 613-636.
- Brown, D., S. Gluck, and J. Hartwig. 1987. Structure of the novel membrane-coating material in proton-secreting cells and identification as an H^+ ATPase. *J. Cell Biol.* 105:1637-1648.
- Brown, D., P. Weyer, and L. Orci. 1987. Non-clathrin coated vesicles are involved in endocytosis in kidney collecting duct intercalated cells. *Anat. Rec.* 218:237-242.
- Brown, D., S. Hirsch, and S. Gluck. 1988. An H^+ ATPase in opposite plasma membrane domains in kidney epithelial cell subpopulations. *Nature (Lond.)* 331:622-624.
- Burg, M., and N. Green. 1977. Bicarbonate transport by isolated perfused rabbit proximal convoluted tubules. *Am. J. Physiol.* 233:F307-F314.
- Cannon, C., J. van Adelsberg, S. Kelly, and Q. Al-Awqati. 1985. Carbon dioxide-induced exocytotic insertion of H^+ pumps in turtle-bladder luminal membrane: role of cell pH and calcium. *Nature (Lond.)* 314: 443-446.
- Cosson, P., I. de Curtis, J. Pouyssegur, G. Griffiths, and J. Davoust. 1989. Low cytoplasmic pH inhibits endocytosis and transport from the trans-golgi network to the cell surface. *J. Cell Biol.* 108:377-387.
- Dani, C., J. M. Blanchard, M. Piechaczyk, S. El Sabouty, L. Marty, and P. Jeanteur. 1984. Extreme instability of myc mRNA in normal and transformed human cells. *Proc. Natl. Acad. Sci. USA.* 81:7046-7050.
- Daukas, G., and S. H. Zigmond. 1985. Inhibition of receptor-mediated but not fluid-phase endocytosis in polymorphonuclear leukocytes. *J. Cell Biol.* 101:1673-1679.
- Dobyan, D. C., and R. E. Bulger. 1982. Renal carbonic anhydrase. *Am. J. Physiol.* 243:F311-F324.
- Drenckhahn, D., K. Schultze, D. P. Allen, and V. Bennett. 1985. Colocalization of band 3 with ankyrin and spectrin at the basal membrane of intercalated cells in the rat kidney. *Science (Wash. DC)* 230:1287-1289.
- Gluck, S., C. Cannon, and Q. Al-Awqati. 1982. Exocytosis regulates urinary acidification by rapid insertion of proton pumps into the luminal membrane. *Proc. Natl. Acad. Sci. USA.* 79:4327-4331.
- Kaissling, B., and W. Kriz. 1979. Structural analysis of the rabbit kidney. *Adv. Anat. Embryol. Cell Biol.* 56:1-123.
- Koeppen, B. M., B. A. Biagi, and G. H. Giebisch. 1983. Intracellular microelectrode characterization of the rabbit cortical collecting duct. *Am. J. Physiol.* 244:F35-F47.
- LeHir, M., B. Kaissling, B. M. Koeppen, and J. B. Wade. 1982. Binding of peanut lectin to specific epithelial cell types in kidney. *Am. J. Physiol.* 242:C117-C120.
- Lombard, W. E., J. P. Kokko, and H. R. Jacobson. 1983. Bicarbonate transport in cortical and outer medullary collecting tubules. *Am. J. Physiol.* 244:F289-296.
- Lotspeich, W. D. 1967. Metabolic aspects of acid-base change. *Science (Wash. DC)* 155:1066-1075.
- Madsen, K. M., and C. C. Tisher. 1986. Structural-functional relationships along the distal nephron. *Am. J. Physiol.* 250:F1-F15.
- McKinney, T. D., and M. Burg. 1977. Bicarbonate transport by rabbit cortical collecting tubules. *J. Clin. Invest.* 60:766-768.
- McKinney, T. D., and M. B. Burg. 1978. Bicarbonate absorption by rabbit cortical collecting tubules *in vitro*. *Am. J. Physiol.* 234:F141-F145.
- Ridderstrale, Y., M. Kashgarian, B. Koeppen, G. Giebisch, D. Stetson, T. Ardito, and B. Stanton. 1988. Morphological heterogeneity of the rabbit collecting duct. *Kidney Int.* 34:655-670.
- Satlin, L. M., and G. J. Schwartz. 1987. Postnatal maturation of rabbit renal collecting duct: intercalated cell function. *Am. J. Physiol.* 253: F622-F635.
- Schuster, V. L., S. M. Bonsib, and M. L. Jennings. 1986. Two types of collecting duct mitochondria-rich (intercalated) cells: lectin and band 3 cytochemistry. *Am. J. Physiol.* 251:C347-C355.
- Schwartz, G. J., and Q. Al-Awqati. 1985. Carbon dioxide causes exocytosis of vesicles containing H^+ pumps in isolated perfused proximal and collecting tubules. *J. Clin. Invest.* 75:1638-1644.
- Schwartz, G. J., J. Barasch, and Q. Al-Awqati. 1985. Plasticity of func-

- tional epithelial polarity. *Nature (Lond.)* 318:368-371.
28. Schwartz, G. J., L. Satlin, and J. E. Bergmann. 1988. Fluorescent characterization of collecting duct cells: a second H⁺ secreting type. *Am. J. Physiol.* 255:F1003-F1014.
 29. Snedecor, G. W., and W. G. Cochran. 1973. *Statistical Methods*. 6th ed. The Iowa State University Press, Ames, Iowa. 120-134; 258-298.
 30. Star, R. A., M. B. Burg, and M. A. Knepper. 1985. Bicarbonate secretion and chloride absorption by rabbit cortical collecting ducts. Role of chloride/bicarbonate exchange. *J. Clin. Invest.* 76:1123-1130.
 31. Van Adelsberg, J., and Q. Al-Awqati. 1986. Regulation of cell pH by Ca²⁺-mediated exocytotic insertion of H⁺-ATPases. *J. Cell Biol.* 102:1638-1645.
 32. Verlander, J. W., K. M. Madsen, and C. C. Tisher. 1987. Effect of acute respiratory acidosis on two populations of intercalated cells in rat cortical collecting duct. *Am. J. Physiol.* 253:F1142-F1156.
 33. Wade, J. B., R. G. O'Neil, J. L. Pryor, and E. L. Boulpaep. 1979. Modulation of cell membrane area in renal collecting tubules by corticosteroid hormones. *J. Cell Biol.* 81:439-445.